AIMS Materials Science, 13(2): 223–239.
DOI: 10.3934/matersci.2026013
Received: 27 September 2025
Revised: 21 January 2026
Accepted: 06 February 2026
Published: 04 March 2026

https://www.aimspress.com/journal/Materials

Research article

Mechanical compression behavior of reinforced and unreinforced thermoplastic film materials as high-performance core layer for semi-finished sandwich products

Tony Weber*, Kurt Böhme and Maik Gude

Institute of Lightweight Engineering and Polymer Technology, TUD Dresden University of Technology, National, Dresden, Germany

* **Correspondence:** Email: tony.weber@tu-dresden.de; Tel: +49-351-463-42498.

Abstract: Thermoplastic honeycomb cores for sandwich structures offer, in addition to high stiffness and low weight, further advantages such as recyclability, chemical resistance, and suitability for large-scale processing. These properties, combined with the broad range of characteristics offered by high-performance thermoplastics such as polyetherimide (PEI), polyphenylene sulfide (PPS), and polyether ether ketone (PEEK), make these materials promising for use in the aerospace industry. With this focus, this paper examined PEI films and carbon fiber-reinforced non-woven materials with PEI and PPS matrices to assess their potential as thermoplastic cores in sandwich structures. Assessing the performance of new material combinations requires adapted testing methods, since conventional characterization of sandwich structures is complex due to their multi-layered nature, especially with regard to the structured core layer. This work introduces a simplified test method for determining the compressive stiffness of film-like and paper-like non-woven thermoplastic core materials. The approach is based on curved compression tests at the coupon level and complemented by in situ computed tomography (CT) analysis of the thermoplastic sandwich at the substructure level, enabling the extraction of mechanical properties and the evaluation of failure mechanisms. Using ThermHex® honeycombs as an example and in comparison to Nomex® structures, the study demonstrates that thermoplastic sandwich semi-finished products hold high potential for efficient, sustainable, and high-performance lightweight applications in aviation.

Keywords: honeycomb; thermoplastic; films; non-wovens; mechanical testing; aerospace

1. Introduction

Sandwich structures based on honeycomb cores have long been used in aviation. These are primarily used for bending-loaded components in the secondary structure, such as floor panels, separation panels, and cladding panels, which are characterized by high specific stiffness. Currently, such structures are made of a core material, mainly phenol-impregnated aramid papers, so-called Nomex® honeycombs, and a cover layer made of semi-finished products with continuous fibers. The aviation industry places extremely high demands on such structures. They must have outstanding mechanical properties and be thermal resistant and flame retardant, durable, damage-resistant, and repairable [1–3]. Although fiber-reinforced plastics offer numerous options for varying the outer layers, the choice of approved materials for the sandwich core is limited by strict aviation guidelines. The efficiency of manufacturing processes for honeycomb structures based on thermoplastic films makes high-performance plastics interesting for aviation applications while fulfilling their high demands, such as thermal resistance. In addition to achieving more efficient production, which is in line with the manufacturer's economic goal due to the predicted sharp increase in passenger volumes [4,5], the aspect of sustainability by using thermoplastic materials and fiber materials must also be taken into account.

Characterizing semi-finished sandwich products is complex due to their multi-layered structure. Therefore, in several tests (tensile and shear), retaining elements need to be applied to the outer layers using adhesives to ensure proper force application and transmission. With regard to the use of thermoplastic films or paper-like non-woven materials with thermoplastic matrices, the variety of available material combinations makes it necessary to define a potential assessment using simplified test methods for the core material as sheet material. Therefore, this paper focuses on determining the compressive load of the core materials. The basis for this is a test using curved compression, which makes it possible to determine the mechanical characteristics of the core materials under compressive stress for paper-like or non-woven materials. Regarding the evaluation of failure characteristics of the sandwich structure, a compression test is carried out, which is sequentially instrumented using in situ computed tomography (CT). This enables the evaluation of the force-displacement curve, simultaneously with the determination of failure phenomenology for new types of semi-finished sandwich products.

2. Materials and methods

Various semi-finished products are examined here using different mechanical material tests to assess their use as core materials in sandwich structures. At the coupon level, thermoplastic sheet materials (thermoplastic non-woven materials and thermoplastic film materials) are examined and compared in terms of their stiffness, using selected tensile and compression tests. High-performance plastics based on polyphenylene sulphide (PPS) and polyetherimide (PEI) were used as matrix materials for carbon fiber (CF)-reinforced nonwovens. PEI film materials are then used as honeycomb material for further investigations at the substructure level in sandwich composites with continuous glass fiber (GF)-reinforced PEI (PEI/GF) cover layers. The core structure is represented by a ThermHex® folded honeycomb geometry. A thermoset sandwich structure consisting of a Nomex honeycomb core and continuous glass fiber-reinforced epoxy (epoxy/GF) cover layers was selected as the structural reference structure.

For clarity and classification, Figure 1 shows a comparison of the different materials and material levels in relation to the different tests and test levels.

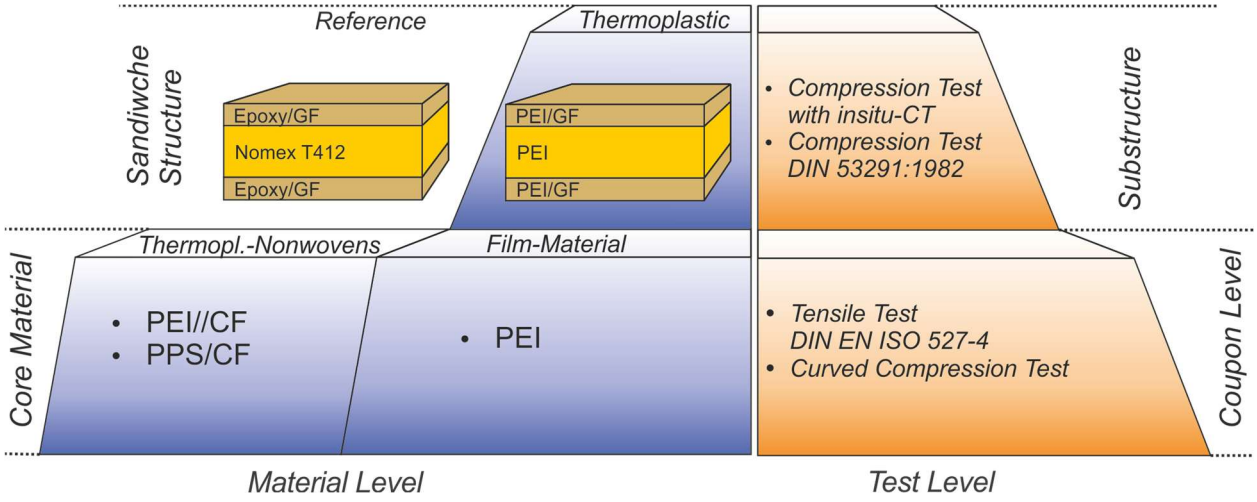

Figure 1. Overview and categorization of the materials examined here and the material tests used.

2.1. Thermoplastic honeycomb materials

Thermoplastic honeycomb materials are innovative semi-finished thermoplastic products with a typical honeycomb structure. Compared with classic honeycomb materials for structurally highly loaded components, they combine the advantages of thermoplastic materials with the structural advantages of the honeycomb structure, which offers high stiffness and strength as well as low weight [6,7].

The specification of the base material defines the subdivision of thermoplastic honeycomb materials, the manufacturing process, and the geometric structure of the honeycombs themselves. In this context, the geometric structure is often subject to the limitations of the manufacturing process. The most common manufacturing processes for thermoplastic honeycombs are extrusion, thermoforming, hot-melt bonding, vacuum deep-drawing, and injection molding. A comprehensive overview of thermoplastic manufacturing processes can be found in [8–10].

Currently, 3D printing possibilities for manufacturing core material, especially for high-performance plastics, are also being investigated. In addition to the structure and topological possibilities, the focus here is on the bonding of the core and cover layer [11,12].

The honeycomb structures examined in this paper are ThermHex® honeycombs, which consist of folded honeycomb core material developed and patented by EconCore NV. The thermoplastic folded core is characterized by hexagonal cells and closed cover layers that allow a fast and reliable bonding of the honeycomb to the core without additional adhesive. The ThermHex® core material can be manufactured continuously in a production line. All production steps can be serially carried out in a rotary process, which enables high production speeds. Starting from a continuous thermoplastic film, the production steps are:

- Forming of semi-hexagonal shapes by thermoforming or vacuum-assisted thermoforming;
- Folding of the semi-hexagonal web to form the honeycomb core;
- Internal bonding of the honeycomb core by thermal melting;
- Lamination of thermoplastic cover layers onto the honeycomb core.

This concept has proven practicable for various types of thermoplastic materials. Thermoplastic folded honeycomb patterns have been produced from various film materials, mainly polypropylene (PP) and polyethylene terephthalate (PET) [13].

Figure 2a schematically shows the honeycomb structure's most specific geometrical parameters. Figure 2b shows a pre-formed non-woven material made from a recycled, semi-finished fiber-reinforced thermoplastic product. The PEI honeycombs examined here as sandwich structures are shown in Figure 2c as a semi-finished product.

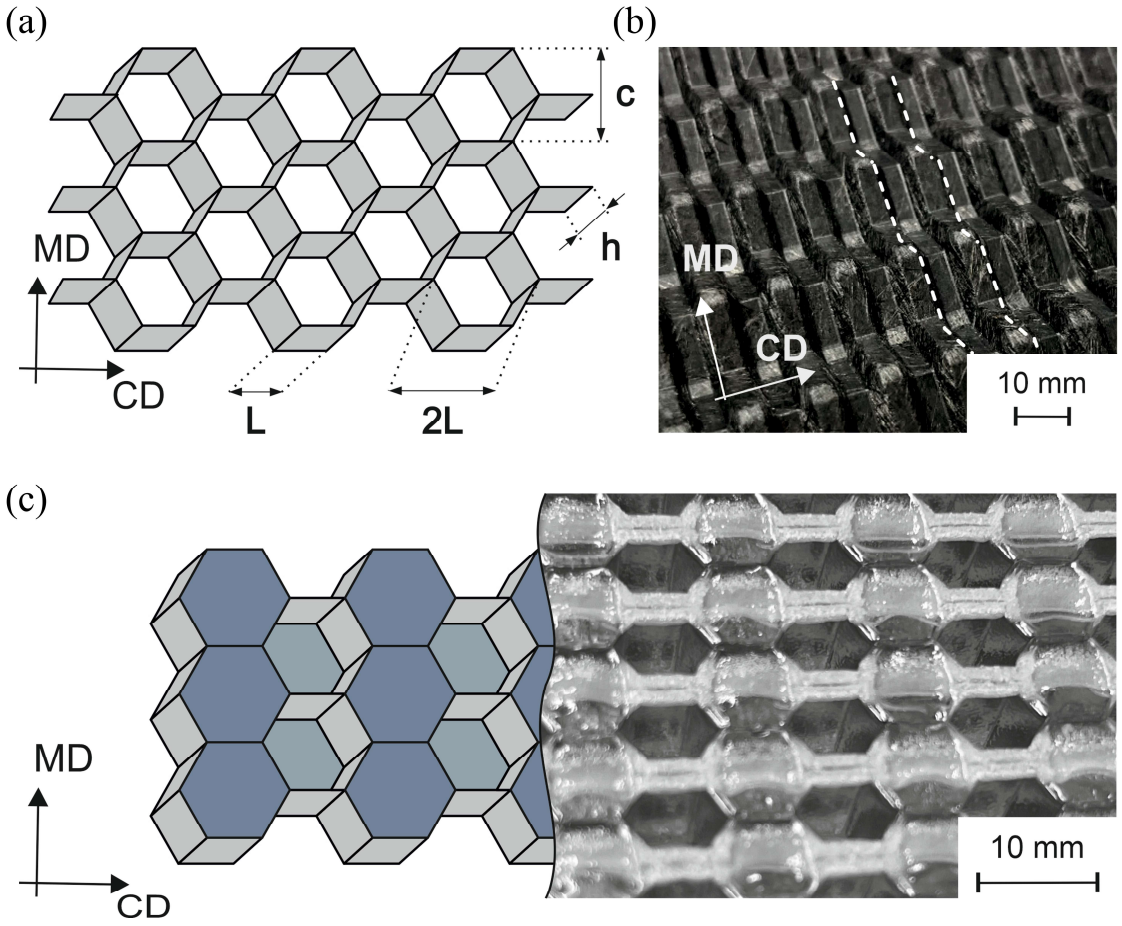

Figure 2. Overview of the main characteristics of thermoplastic honeycombs (MD: manufacturing direction; CD: cross direction). (a) Schematic figure of hexagonal honeycomb structures (h: cell height; c: cell size; L: side length). (b) Pre-formed non-woven material made from recycled semi-finished fibers with uneven surface structure. (c) Schematic figure and photo of ThermHex® PEI honeycomb.

2.2. Semi-finished products and process variations

The use of fiber-reinforced semi-finished products based on recycled carbon fibers as a core material is investigated here with regard to sustainability and in terms of increased specific compressive stiffness [14,15]. Thus, commingled non-woven materials based on chopped fibers are used here. These are composite materials consisting of a mixture of thermoplastic and reinforcing fibers, where fibers and matrix are arranged close to each other. An even distribution of fibers and

thermoplastic material in these hybrid materials results in a quasi-homogeneous behavior [16–18]. The non-woven materials are available on a roll in a dry or unconsolidated state and are easy to handle. In addition to the mechanical properties, this is crucial to ensure further processability into pre-formed honeycomb semi-finished products (see Figure 2b). Process control, especially temperature and pressure as a function of time, is of fundamental importance in molding procedures. In order to produce the semi-finished flow molded product of appropriate quality, the processing ranges are narrow, especially for high-performance thermoplastics [19]. In this paper, a homogeneous PEI film material was also used in addition to hybrid materials based on recycled carbon fibers in combination with PEI and PPS thermoplastics. On the one hand, the film material serves as a reference sample for the material tests used; on the other hand, it also demonstrates the potential of thermoplastic honeycomb core materials by analyzing sandwich samples produced using autoclave technology.

Configurations of the used materials, process variants, and parameters are shown in Table 1. The grammages of the semi-finished products range from 222 to 262 g/m^2. Consolidation tests of the materials were carried out by the project partner ThermHex Waben GmbH using three process configurations: stamp forming with hot plates, long-cycle vario-thermal stamping, and stamp forming with upstream infrared heating (IR). A sequential heating and pressing step was assumed for both processes. The consolidation processes differ in the methods used for heating the non-woven fabric: using infrared radiators or indirectly using steel plates heated in a convection oven. In addition to the heating process and its parameters, transferring the hot, melted, flexible, semi-finished product into the press chamber is of central importance in sequential process control. This transfer process is completely bypassed by using heated plates, which provides a process-related advantage when heating the non-woven semi-finished product.

Table 1. Investigated materials and process configurations (PC) of the consolidated non-woven materials.

PC	Material	Grammage (g/m^2)	Thickness (mm)	Processing method	Temp. (°C)	Pressure (bar)
Film material						
1	PEI	222	0.174	Commercial available film		
Thermoplastic non-woven reinforced with recycled carbon fibers						
2	PEI/CF	254	0.230	Stamp forming with hot metal plates	400	108
3	PEI/CF	259	0.200			75
4	PEI/CF	262	0.200			52
5	PPS/CF	259	0.270	Long cycle vario-thermal stamping	IR	13
6	PPS/CF	235	0.270	Stamp forming with IR	IR	60
7	PPS/CF	242	0.270			60
8	PPS/CF	227	0.280			26
9	PPS/CF	228	0.220	Stamp forming with hot metal plates	350	52
10	PPS/CF	231	0.200			52
11	PPS/CF	231	0.190			56
12	PPS/CF	259	0.200			56

Different qualities of the semi-finished product are generated depending on the consolidation process and the set parameters. Examples of the different qualities are shown in the micrographs in Figure 3. Process configuration (PC) 5 (Figure 3a) and PC 11 (Figure 3b) of the PPS/CF variants show different consolidation quality. PC 5 shows many air inclusions and a relatively poorer quality of consolidation. This was, on one hand, caused by the lower pressing pressure. Still, considering the thicknesses of the materials consolidated in the same manufacturing process, it becomes clear that the process itself is subject to restrictions. The heating by means of infrared radiation and the transfer into the press chamber have an inhibiting effect. Figure 3c shows the differences in the fiber distribution across the cross-section of the material of PC 3. Areas with a high accumulation of fibers alternate with thermoplastic matrix areas. However, the consolidation process cannot influence the fiber distribution within the material.

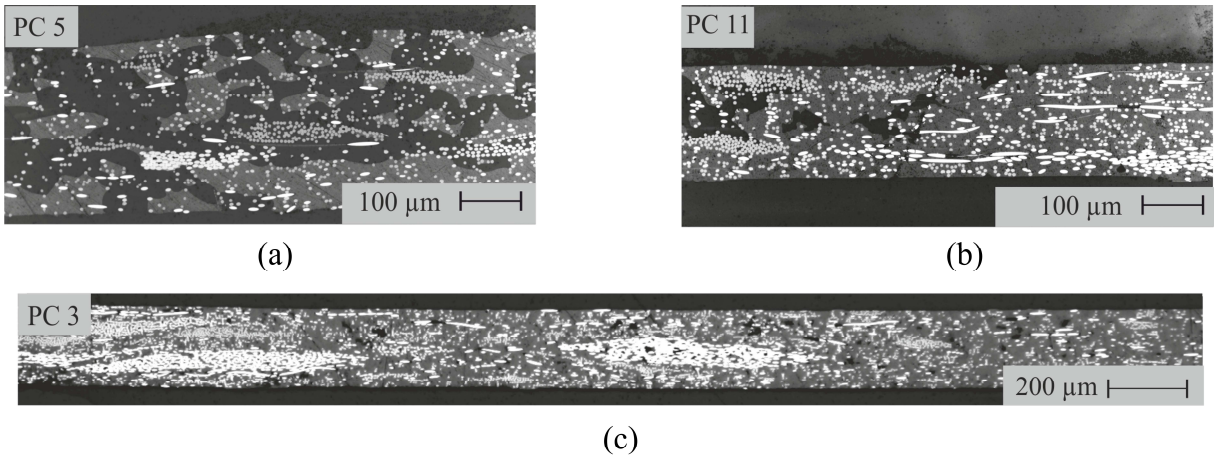

Figure 3. Micrographs of different process configurations: (a) PPS/CF, long cycle vario-thermal stamping; (b) PPS/CF, stamp forming with hot metal plates; (c) PEI/CF, stamp forming with hot metal plates.

2.3. Experimental tests at the coupon level on films and non-woven materials

Different test methods are necessary to determine specific mechanical behaviors for the comprehensive characterization of paper or web-like materials, as required for continuum mechanical modeling. A large number of test devices and standardized test methods are available for this purpose; for this group of materials, such methods have been developed and standardized primarily for the requirements of the paper processing industry. While some of these methods are suitable for the quantitative determination of characteristic mechanical properties, others are mainly used for the qualitative comparison of different paper grades. Figure 4, based on Bugiel [20], provides an overview of the existing approaches to solve stability failure and presents various test methods developed for testing paper under compressive load. For structures with net-like reinforcement, the free path length in the test plays a vital role with regard to the selection of suitable mechanical tests.

Investigating the mechanical properties of paper or web-like materials under compressive load within the membrane plane poses a particular challenge due to the low material thickness. Even small load paths in the range of a few millimeters often do not lead to material failure but to a stability failure of the sample. Various test methods have been developed in recent decades to address this problem. Many of these are geared toward the requirements of the paper production industry, which is less

interested in detailed mechanical characterization than in practical methods for comparing different paper qualities [21].

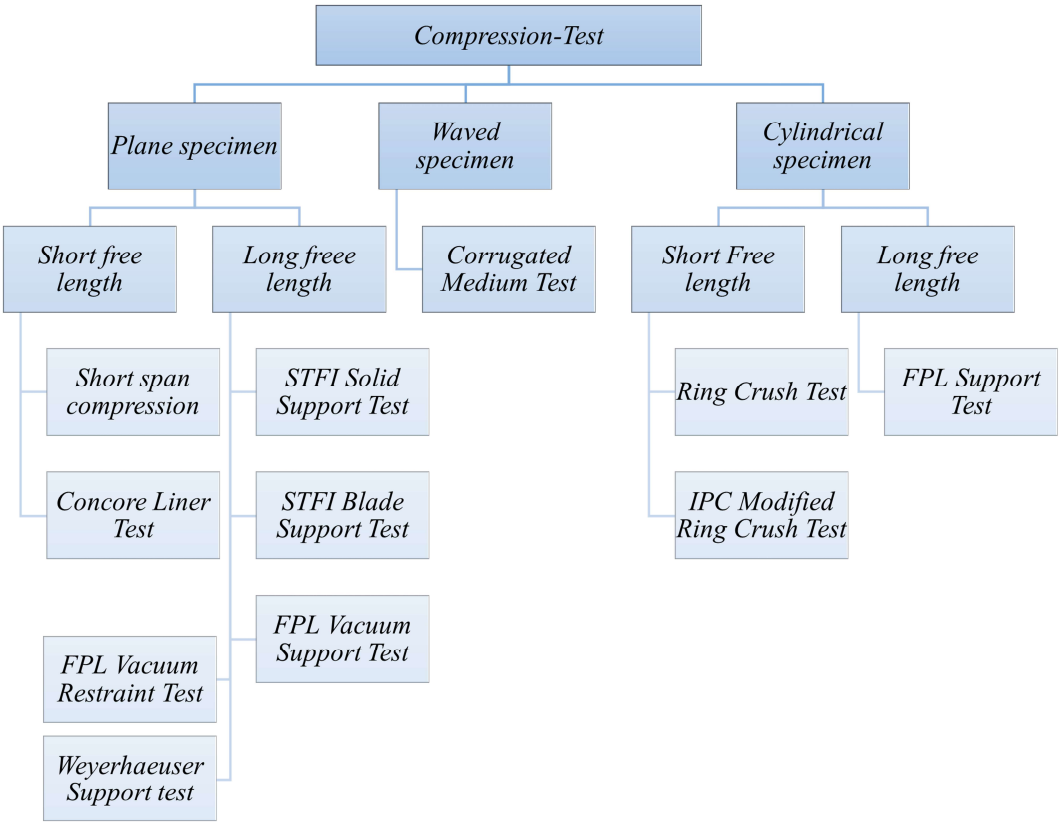

Figure 4. Overview of test methods for compressive load on thin non-woven and paper materials (Reproduced from Ref. [20] with permission).

2.3.1. Curved compression test

In the investigations carried out here, the focus is on characterizing the stiffness of the materials. Due to its use as a core material in sandwich structures subjected to bending or compression, the characteristic value of the specific compressive stiffness is of primary importance for assessing the potential of different materials. On this subject, Bugiel's work evaluated the advantages and disadvantages of the test methods listed in Figure 4. Using optical measurement technology, a curved compression test device was derived for determining the stress–strain curve. This test method and the setup used in this paper are shown in detail in Figure 5. Tests were carried out using a universal testing machine with a customized load cell and a stereo digital image correlation (DIC) system. The test fixture with a normalized length (l_{CT}) of 80 mm and an entry angle (α_{CT}) of 20° was used to test the non-woven materials (see Figure 5a). The test specimens had dimensions of 83.5 × 15 mm and were cut out of the consolidated semi-finished product using a cutter with an ultrasonic knife. Figure 5b shows the main elements of the test fixture, consisting of the test frame with clamping jaws (1, 2), the support plates (3), and the test specimen (4). To achieve a better support effect for the large number of material configurations used, the tests were carried out with additional support tongues (5) (see Figure 5c). Figure 5d shows the evaluation range of the optical strain measurements. The strain

represents a stochastic mean value of the recorded strain facets of the analyzed range (highlighted in green) [22]. The number of support points for strain determination in this area (approximately 3 × 8 mm) is approximately 250. Image acquisition is force-synchronized to determine the stress–strain curves.

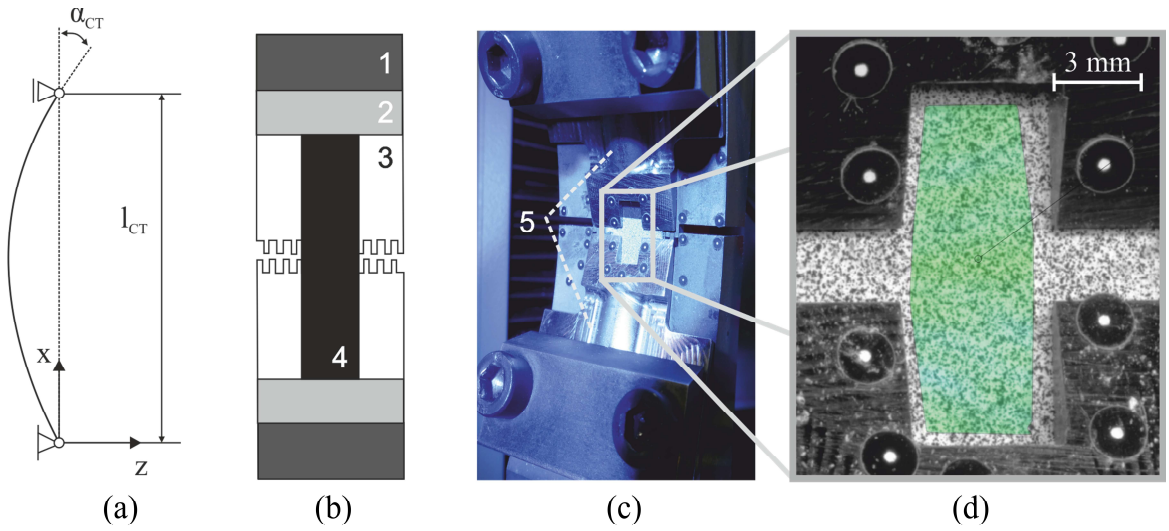

Figure 5. Methodology of the curved compression test fixture with optical strain recording: (a) Definition of the bending line; (b) essential elements of the test fixture: clamping jaws (1, 2), support plates (3), and test specimen (4); (c) test setup with support tongues (5); and (d) detailed image with evaluation area (green).

2.3.2. Tensile test

The tensile tests were carried out on a universal tensile testing machine with pneumatic clamping jaws, as shown in Figure 6. In addition to the integrated force measurement, the non-contact 2D video extensometer was selected to record the elongation of the sample. The image shows the testing machine with the clamped sample. The test parameters were selected in accordance with DIN EN ISO 527-4. Due to the raw material and comparability with the compression tests, the test specimen dimensions were defined as a width of 15 mm and a length of 180 mm. Tensile tests were performed with a preload of 5 N. The test speed was set to 2 mm/min, while a reduced crosshead speed of 1 mm/min was used for the determination of tensile modulus. The initial gauge length was 85 mm. The tensile modulus was evaluated within a strain range from 0.05% to 0.25%.

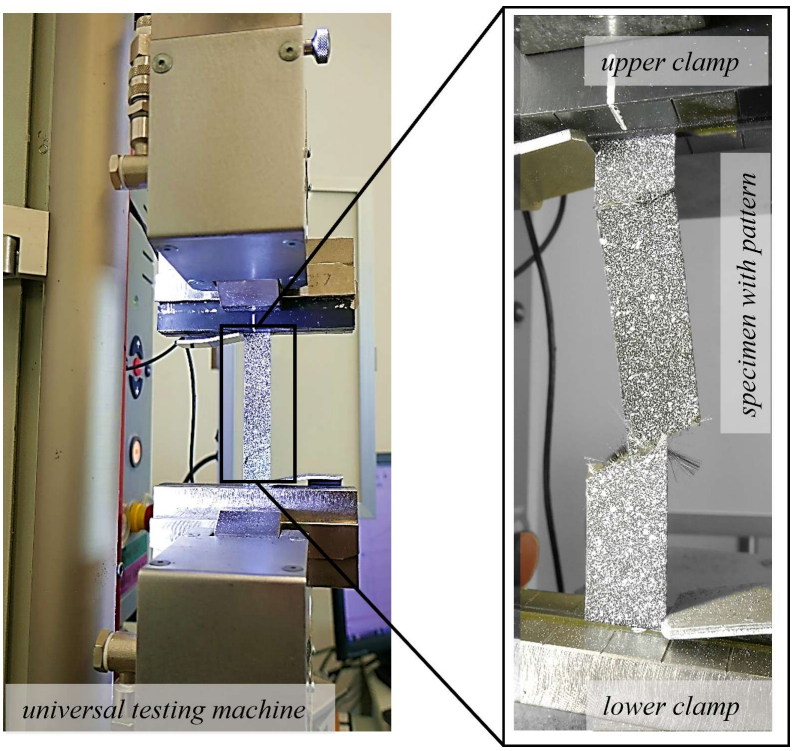

Figure 6. Tensile test on a non-woven material and test specimen with a stochastic pattern for optical strain measurement after failure.

3. Results

3.1. Coupon-level

Figure 7 shows the results of the experimental tests as a bar chart with error bars and the individual values of the stiffness and specific stiffness in relation to the weight per unit area. The arithmetic mean is shown. The error bars show the range mean ± 1.5 standard errors (SE) and indicate the uncertainty of the mean. The median line marks the median of the data. Individual measured values that lie significantly outside the other values are also shown as outliers. The diagram shows all the materials listed in Table 1 according to the corresponding number. Both the tensile (T) and compression (C) values are displayed. The line in the background represents the characteristics of the reference (Nomex® T412 paper) under compressive stress [23].

The results show a considerable scatter, reflected in the error bars' width. This indicates a substantial variability within the samples, possibly caused by material inhomogeneities, systematic errors in the metrological determination of the characteristic values, and consolidation fluctuations. As all test specimens were taken from only one consolidated panel, process-related consolidation fluctuations can be largely excluded. Regarding the evaluation of the quality of the measurement method for determining compression parameters, a reference should be made to the results and the scatter of the tensile tests, which show a similarly strong scatter of the characteristic values. Furthermore, the quality of the measurement method is confirmed by the low scatter band and the characteristic values determined for the homogeneous film material PEI (PC 1). As a result of this and the fact that the tensile test used is an established test method for such investigations, it can be assumed that the majority of the variation can be attributed to inhomogeneities in the flow material itself. These

inhomogeneities mainly concern local differences in fiber density, fluctuating surface mass, areas with fiber accumulations or thinning, and also differences in the orientation of the fiber material of the semi-finished product. Due to the use of similar grammages, the differences in the absolute and specific stiffness of the non-woven materials analyzed are marginal. A comparison with the reference or homogeneous material shows that the specific stiffness is the decisive factor, especially for use as a high-performance core material.

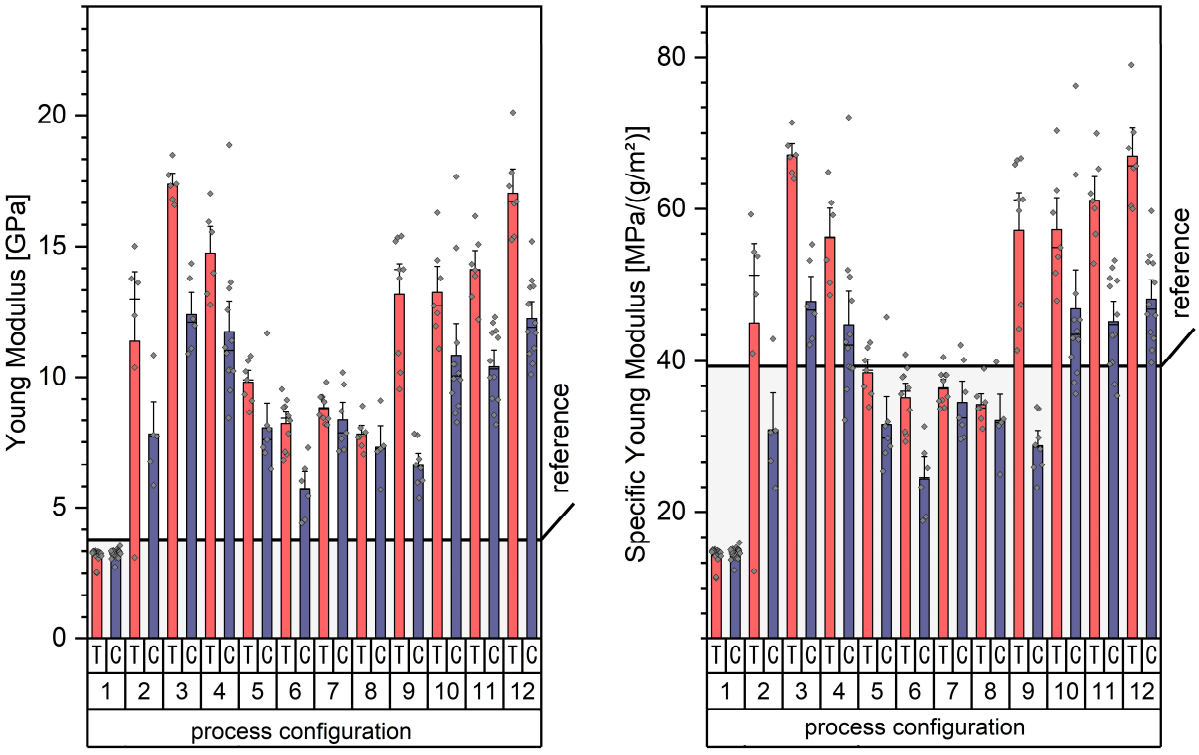

Figure 7. Results of the tensile (T) and compression (C) stiffness tests: Young's modulus and specific modulus related to the grammage of the specimen in regard to the reference (Nomex® T412 paper).

In addition to the wide variation in the stiffness results and the relatively low specific stiffness values of the pure PEI film, the difference between the compressive and tensile stiffness of the non-woven materials is particularly pronounced. Exceptions are the material groups No. 5, 6, 7, and 8, which generally show a lower stiffness level. This can be clearly attributed to the manufacturing process. Both the cross-sectional fiber distribution, shown in the micrograph in Figure 3a, and the measured material thicknesses indicate a low consolidation quality, which caused lower stiffness under tensile stress. This difference is less pronounced under compressive load, possibly due to the higher material thickness and its influence on the surface inertia.

The comparison of the PEI-CF materials (PC 2, 3, 4) with the homogeneous PEI Variant (PC 1) shows that the influence of the fiber reinforcement is clearly visible and results in significantly higher stiffnesses. With the same grammage, the thickness of the consolidated material can serve as an indicator of the consolidation quality, which explains the lower characteristic values of material PC 2. Stiffnesses at a similarly high level were measured for the fleeces with PPS matrix (PC 9, 10, 11, 12).

Both the well-consolidated fleeces with PEI matrix and those with PPS matrix achieve higher average stiffness values under compressive load than the reference material.

3.2. Substructure level

To transfer the potentials shown in Figure 7 to high-performance semi-finished sandwich products, PEI ThermHex® honeycombs, based on the PEI films investigated, were combined with PEI/GF organosheet cover sheets to form semi-finished sandwich products. These semi-finished products were produced in a hot lamination process using vacuum compression in the autoclave. The consolidated cover layers were bonded to the honeycomb structure using a coupling layer under pressure and temperature. The paper focuses mainly on the failure modes of the thermoplastic core structure under compressive load. These investigations are analyzed by means of in situ CT during load tests. This special examination method is explained in detail in [24], and the respective test setup is shown in Figure 8. The main difference to the setup within a conventional testing machine is the use of coupling plates between the test specimen and the metallic load string. This serves to counteract the formation of artefacts during X-ray image reproduction to achieve better contrasts and a detailed representation of the honeycomb structure. Furthermore, the load curve must be interrupted at defined levels due to the time required for the CT scan of the test specimen. For this purpose, three displacement/force levels were defined: at low load, at load before the force maximum, and significantly after the force maximum.

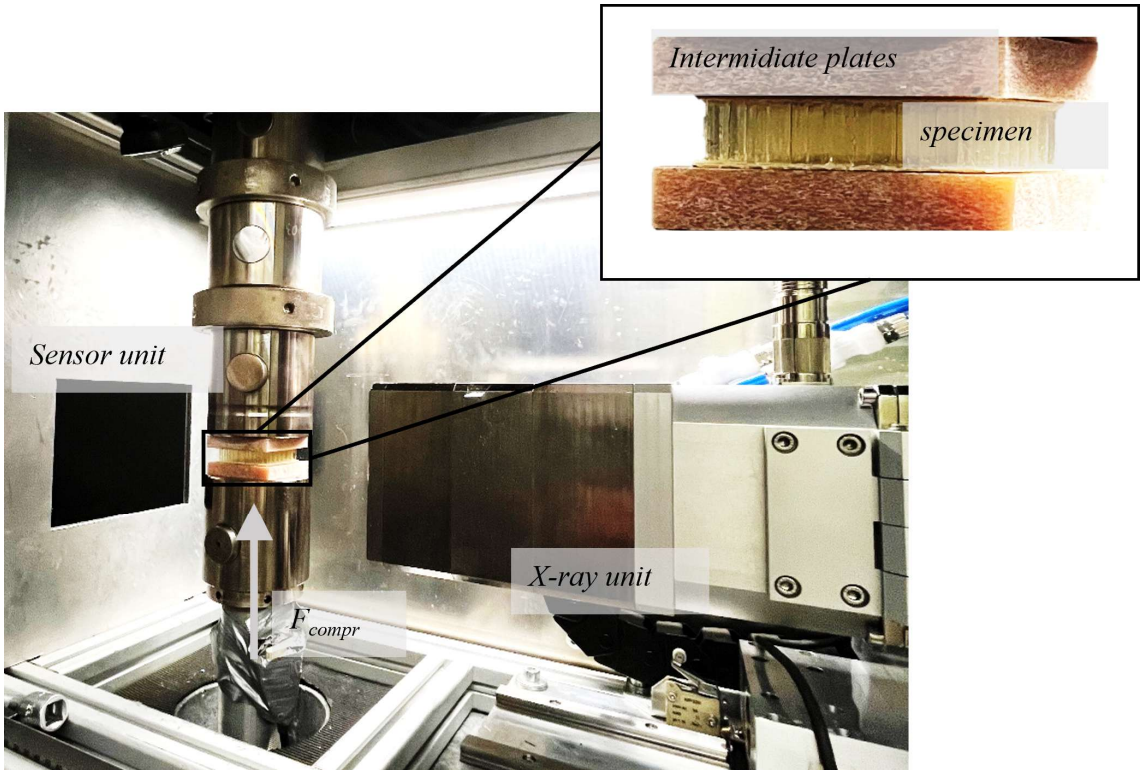

Figure 8. Test setup for compression tests of honeycomb structures within an in situ CT testing machine.

The load levels and the corresponding force-displacement curves are shown in comparison with the results of the standard tests in Figure 9. The standard tests were carried out in accordance with

DIN 53291:1982, and the in situ CT tests are based on this standard. Thus, the square base of the specimen has a side length of 50 mm, and the specimen height is approximately 11.5 mm. The force-displacement curves of the standard specimens show a very homogeneous characteristic, except for one specimen (Figure 9a). The relationship between edge length and cell size can also explain this deviation. If a single cell is damaged, the influence on the structural performance of the entire specimen is not insignificant. Compared to the standard specimens, the in situ CT specimen shows a lower initial stiffness but a higher maximum force. This behavior can be caused by the relaxation times during the single CT measurements. Stress relaxation reduces the mechanical stress under constant load. This effect, caused by molecular rearrangement and creep processes, particularly occurs in the first few minutes (source: plastics testing). The increased maximum force contradicts the influence of relaxation, so it is more a question of structural and manufacturing influences on the overall structure.

Figure 9b compares the thermoplastic PEI sandwich structure (core 2) with a typical aerospace sandwich structure. This structure (core 1) is made from the commercially available thermoset core material Coremaster® C1 (C1-3.2-48, core 1), manufactured from Nomex®T412 paper and two cover layers of glass epoxy prepreg, each to a total structure thickness of approximately 11 mm. The maximum compressive force of the thermoset structure is higher than that of the thermoplastic version. In addition to the pure material comparison shown in Figure 7, the different honeycomb structures due to different manufacturing processes must also be taken into account.

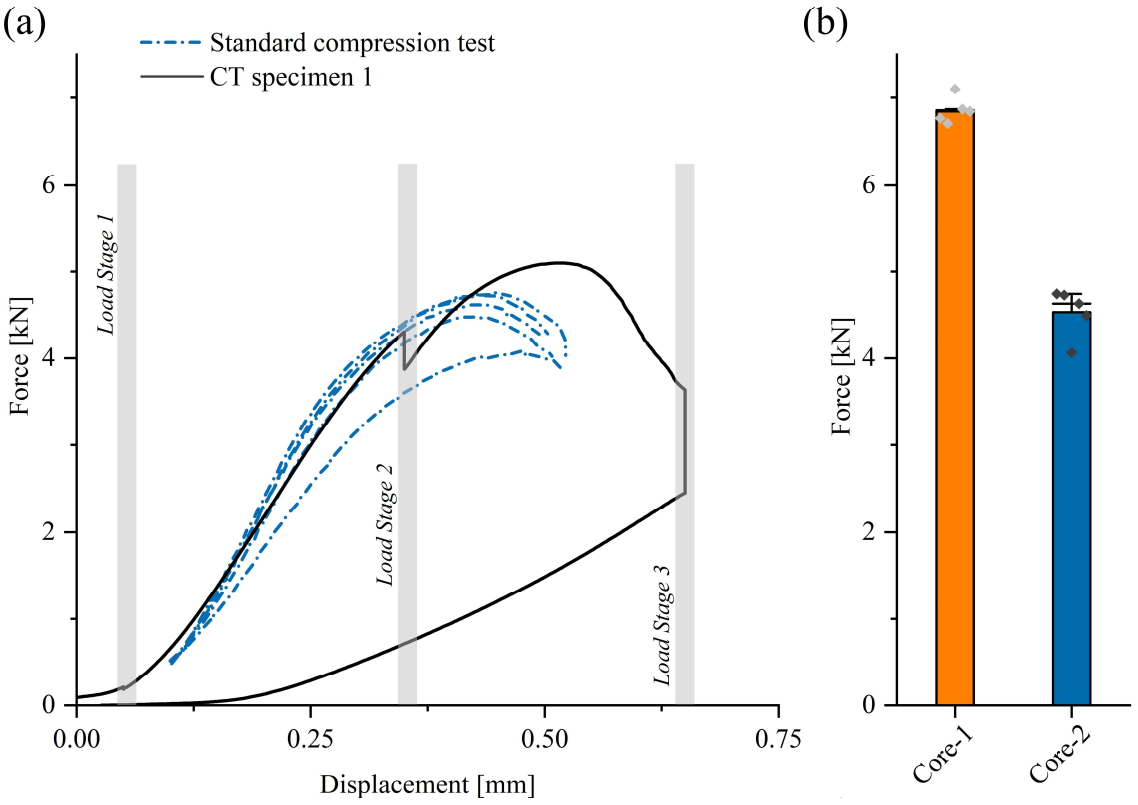

Figure 9. Results of the compression tests: (a) force displacement curve of the standard compression tests and the in situ CT compression test; (b) comparison of the maximum compression forces from the 50 × 50 mm compression tests for the two investigated core materials.

The behavior of the structural failure of the thermoplastic honeycomb structure detected in the in situ CT is shown in Figure 10. In addition to the selected sections lateral to the base surface, the top view normal to the sheet plane is also shown. These images also show the manufacturing-related difference in the structure in the machine direction (MD) and the cross direction (CD) [8]. The two webs of the ThermHex® structure are clearly visible in the lateral sectional view in the yz-plane.

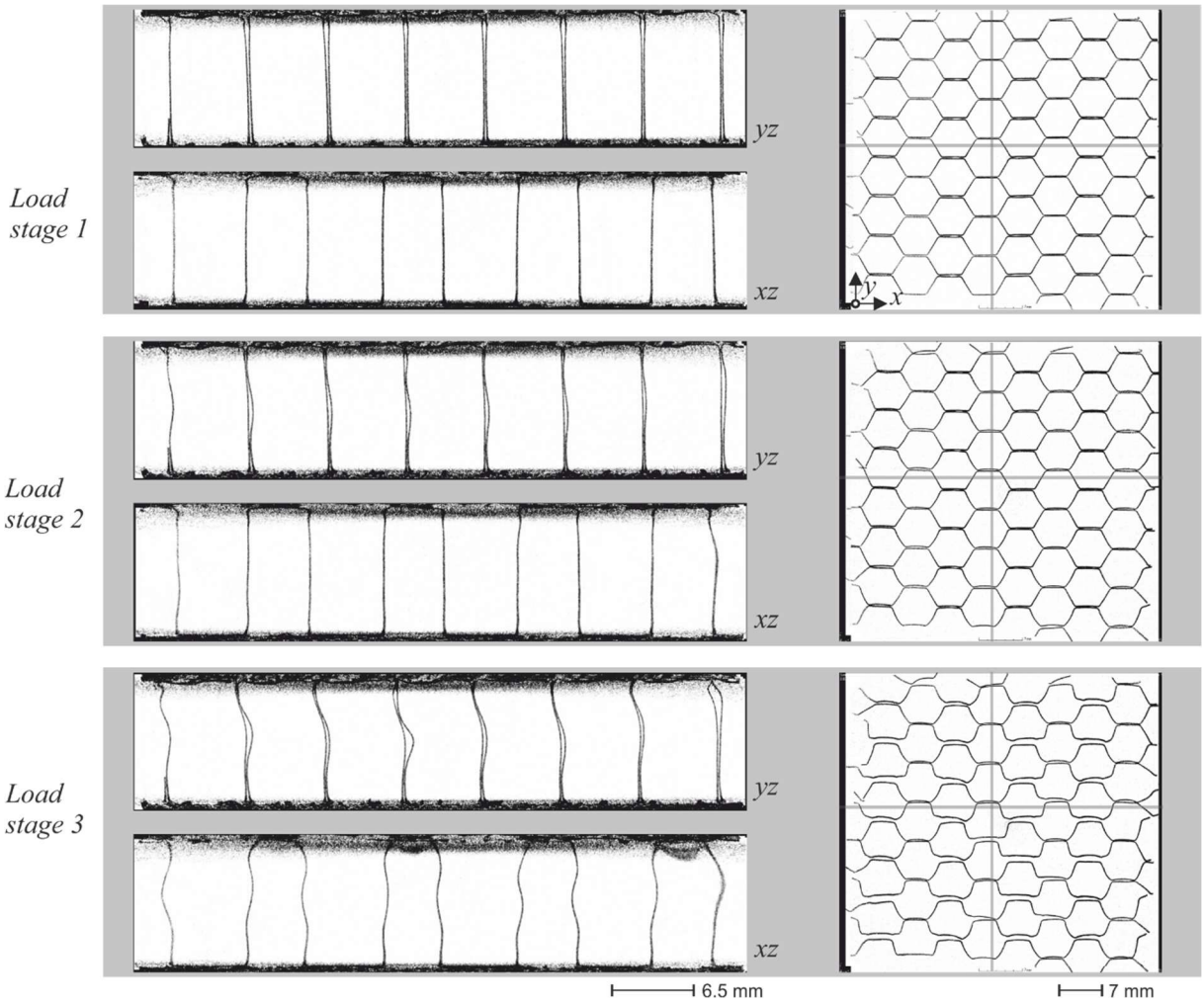

Figure 10. CT images of different load levels for compressive loading of thermoplastic sandwich structures.

The sequence of load stage 1 to load stage 3 shows the progressive stability failure of the honeycomb structure. Two central mechanisms can be observed: the local failure of the side walls, depending on the initial structure, and the global failure of the entire structure (load stage 3).

In the first load stage (stage 1), the quasi-unloaded structure can be seen with slight skewing of individual cell walls. In addition, the slightly different distances between the cell walls in the MD direction can be recognized. The hexagonal arrangement is largely intact, except for the edge area. Increasing the load to stage 2, the local instability rises, with all cell walls transitioning to buckling failure. The cross-sectional images (Figure 10, left) clearly show that the bulging of the side walls increases with rising loads and individual cells become increasingly deformed. The double ridges in the MD direction buckle more than the single ridges. A pronounced double-wave pattern is

recognizable, and the cell walls support each other as they bulge. Thus, the buckling pattern of the sections is relatively homogeneous. This means that all cell walls are similarly stressed. The top view (Figure 10, right) shows a pronounced distortion of individual honeycomb structures. The cells begin to shift sideways, which leads to an inhomogeneous distribution of the load.

A far-reaching collapse of the entire honeycomb structure characterizes the final global failure (load stage 3). In the cross-sectional images, the side walls are severely deformed and show a pronounced wave-like deformation, like a double-S structure. The cells are either considerably compressed or completely collapsed. In the strongly distorted geometry, the originally regular hexagonal cells are no longer recognizable. Instead, the structure shows a wavy, non-homogeneous collapse pattern characterized by local folding zones and displacement of individual cells. Some cell areas have collapsed, while neighboring regions have remained slightly stable. Due to the free edges of the specimen, this uneven deformation is particularly recognizable in the peripheral areas of the structure.

To summarize, the sequence of load stages shows a failure mechanism of thermoplastic honeycomb structures. The initial failure begins with local buckling zones, which expand with increasing load and finally lead to a large-scale structural collapse. The top view in the last load stage illustrates this process through the strongly distorted cell geometry, the wave-shaped deformation patterns, and the relative displacements of the cell walls and cover layers. The buckling behavior of the individual webs clearly characterizes the global failure.

4. Discussion and conclusions

The study shows the mechanical compression behavior of reinforced and unreinforced thermoplastic film and non-woven materials concerning their suitability as a core layer for high-performance sandwich structures. Sandwich structures with thermoset Nomex® honeycomb cores and fiber-reinforced cover layers are used particularly in the aerospace sector due to their high specific stiffness. New manufacturing processes for thermoplastic honeycomb structures offer promising alternatives to conventional core materials. Thermoplastic honeycombs combine structural advantages with sustainability, recyclability, and high production speed.

Various material combinations of recycled CF and high-performance thermoplastics (PEI, PPS) were investigated. The materials were produced using different consolidation processes and tested for compressive strength. The Nomex® T412 paper serves as a reference for both the film material and the honeycomb structure. Experimental investigations show a high scattering of measurement results due to material inhomogeneities and different consolidation qualities. Nevertheless, some reinforced thermoplastic honeycombs are competitive with the mechanical properties of Nomex honeycombs, particularly in terms of specific stiffness under compressive load.

In addition, initial compression tests were carried out on semi-finished sandwich products with PEI-Thermhex® honeycomb cores and glass fiber–reinforced PEI cover layers. The failure of the honeycomb structure was analyzed using in situ CT. The results of this investigation show global failure induced by the global stability failure of the cell walls. On the one hand, compressive stiffness is directly proportional to the critical buckling stress, especially for fiber-reinforced semi-finished products. It is validated as a characteristic parameter for the potential estimation. On the other hand, the competitiveness of homogeneous thermoplastic honeycomb structures for this structural segment is demonstrated.

This group of materials offers enormous potential for use as high-performance core materials for sandwich structures, provided that the manufacturing process for short and long fiber–reinforced thermoplastic semi-finished products can be optimized to ensure consistent material properties. The further processing of semi-finished products into honeycomb structures poses a particular challenge in this regard.

Use of AI tools declaration

The authors declare they have not used Artificial Intelligence (AI) tools in the creation of this article.

Acknowledgments

The authors gratefully acknowledge the financial support of the BMWK within the LuFo V-3 project “TerESa” (20W1720C).

Author contributions

Tony Weber: conceptualization, methodology, validation, data curation, writing the original draft, visualization (Figures); Kurt Böhme: investigations and formal analysis; Maik Gude: resources, writing–review & editing, supervision, funding acquisition.

Conflict of interest

The authors declare no conflict of interest.

References

1. Baker AA, Scott ML (2016) *Composite Materials for Aircraft Structures*, 3 Eds., Reston, VA: American Institute of Aeronautics and Astronautics Inc. https://doi.org/10.2514/4.103261
2. Ma W, Elkin R (2022) *Sandwich Structural Composites: Theories and Practices*, 1 Ed., Boca Raton, FL: CRC Press. https://doi.org/10.1201/9781003035374
3. Schürmann H (2007) *Konstruieren mit Faser-Kunststoff-Verbunden*, 2 Eds., Heidelberg: Springer Berlin. https://doi.org/10.1007/978-3-540-72190-1
4. Boeing (2022) Commercial Market Outlook 2022–2041. Available from: https://www.boeing.com/content/dam/boeing/boeingdotcom/market/assets/downloads/CMO_2022_Report_FINAL_v02.pdf (accessed on 16 May 2024).
5. Airbus (2025) Airbus Global Market Forecast 2025–2044. Available from: https://www.airbus.com/en/products-services/commercial-aircraft/global-market-forecast (accessed on 23 July 2025).
6. Mcgarva LD (2002) *Thermoplastic Composite Sandwich Components: Experimental and Numerical Investigation of Manufacturing Issues*, Stockholm, Sweden: Royal Institute of Technology.
7. Carlsson LA, Kardomateas GA (2011) *Structural and Failure Mechanics of Sandwich Composites*, Dordrecht: Springer Netherlands. https://doi.org/10.1007/978-1-4020-3225-7

8. Philipp Bratfisch J, Vandepitte D, Pflug J, et al. (2005) Development and validation of a continuous production concept for thermoplastic honeycomb, In: Thomsen O, Bozhevolnaya E, Lyckegaard A, *Sandwich Structures 7: Advancing with Sandwich Structures and Materials*, Dordrecht: Springer. https://doi.org/10.1007/1-4020-3848-8_77
9. Fan X, Verpoest I, Pflug J, et al. (2009) Investigation of continuously produced thermoplastic honeycomb processing—Part I: Thermoforming. *J Sandw Struct Mater* 11: 151–178. https://doi.org/10.1177/1099636208098216
10. Latsuzbaya T, Middendorf P, Voelkle D, et al. (2024) Thermomechanical analysis of thermoplastic mono-material sandwich structures with honeycomb core. *J Compos Sci* 8: 18. https://doi.org/10.3390/jcs8010018
11. Martin RG, Johansson C, Tavares JR, et al. (2024) CF/PEEK skins assembly by induction welding for thermoplastic composite sandwich panels. *Compos Part B Eng* 284: 111676. https://doi.org/10.1016/j.compositesb.2024.111676
12. Jiang H, Jia R, Aiyiti W, et al. (2023) Infill strategies for 3D-printed CF-PEEK/HA-PEEK honeycomb core-shell composite structures. *J Manuf Process* 92: 338–349. https://doi.org/10.1016/j.jmapro.2023.02.058
13. ThermHex (2025) Thermoplastische Polypropylen-Wabenkerne und Sandwichplatten für Leichtbauanwendungen und Verbundwerkstoffe. Available from: https://thermhex.com/de (accessed on 1 June 2025).
14. Pakdel E, Kashi S, Varley R, et al. (2021) Recent progress in recycling carbon fibre reinforced composites and dry carbon fibre wastes. *Resour Conserv Recycl* 166: 105340. https://doi.org/10.1016/j.resconrec.2020.105340
15. Pimenta S, Pinho ST (2011) Recycling carbon fibre reinforced polymers for structural applications: Technology review and market outlook. *Waste Manage* 31: 378–392. https://doi.org/10.1016/j.wasman.2010.09.019
16. Wiegand N, Mäder E (2017) Commingled yarn spinning for thermoplastic/glass fiber composites. *Fibers* 5: 26. https://doi.org/10.3390/fib5030026
17. Patou J, Bonnaire R, De Luycker E, et al. (2019) Influence of consolidation process on voids and mechanical properties of powdered and commingled carbon/PPS laminates. *Compos Part A Appl Sci Manuf* 117: 260–275. https://doi.org/10.1016/j.compositesa.2018.11.012
18. Mankodi H, Patel P (2009) Study the effect of commingling parameters on glass/polypropylene hybrid yarns properties. *Autex Res J* 9: 70–73. https://doi.org/10.1515/aut-2009-090303
19. Minupala VK, Zscheyge M, Glaesser T, et al. (2024) Numerical modelling of the thermoforming behaviour of thermoplastic honeycomb composite sandwich laminates. *Polymers* 16: 594. https://doi.org/10.3390/polym16050594
20. Bugiel A (2020) Ein Beitrag zur mechanischen Charakterisierung und numerischen Simulation von Aramid-Papier für Luftfahrtanwendungen. TUD Dresden University of Technology, Dresden, Germany. Available from: https://tud.qucosa.de/api/qucosa%3A74255/attachment/ATT-0/.
21. Bugiel A, Hähnel F, Wolf K (2018) *Erhöhung der Zuverlässigkeit von hochbelasteten Leichtbau-Faserverbund-Sandwich-Strukturen durch abgesicherte Nachweismethoden zur Bewertung der Schadenstoleranz*, Technische Universität Dresden, Fakultät Maschinenwesen, Institut für Luft- und Raumfahrttechnik, Lehrstuhl für Luftfahrzeugtechnik: Dresden.

22. Gottwald R (2015) Beitrag zur analytischen, numerischen und experimentellen Kerbspannungsanalyse endlich berandeter anisotroper Mehrschichtverbunde, TUD Dresden University of Technology, Dresden, Germany.
23. Hähnel F (2016) *Ein Beitrag zur Simulation des Versagens von Honigwaben aus Meta-Aramid-Papier in schlagbelasteten Sandwich-Strukturen*, Aachen: Shaker Verlag. Available from: www.shaker.de/shop/978-3-8440-4366-2.
24. Köhler D, Kupfer R, Troschitz J, et al. (2021) In situ computed tomography-analysis of a single-lap shear test with clinch points. *Materials* 14: 1859. https://doi.org/10.3390/ma14081859

AIMS Press